ELSEVIER

Journal of Organometallic Chemistry 552 (1998) 255–263

Journal of Organometallic Chemistry

Carbyne complexes of the group 6 metals containing 1,4,7-triazacyclononane and its 1,4,7-trimethyl derivative

Fu-Wa Lee, Michael Chi-Wang Chan, Kung-Kai Cheung, Chi-Ming Che *

Department of Chemistry, The University of Hong Kong, Pokfulam Road, Hong Kong, China

Received 21 July 1997

Abstract

Interaction of $Cl(CO)_2py_2M{\equiv}CPh$ (M = Mo, W) with 1,4,7-trimethyl-1,4,7-triazacyclononane (Me_3TACN) in THF, followed by metathesis using $NaBPh_4$ in aqueous medium, readily afford $[(Me_3TACN)M(CO)_2({\equiv}CPh)]BPh_4$ (M = Mo (**1a**), W (**2**)). $[(TACN)Mo(CO)_2({\equiv}CPh)]BPh_4$ (**1b**) is similarly prepared using the molybdenum precursor and 1,4,7-triazacyclononane (TACN). Complex **1a**, **1b** and **2** are stable in the presence of concentrated hydrochloric acid at room temperature. The crystal structures of **1a** and **2** both show that the three nitrogen atoms of Me_3TACN are not equidistant from the metal centre as a consequence of the different *trans* influences of the carbyne and carbonyl groups. Complexes **1a**, **1b** and **2** exhibit intense absorption bands at 320–340 nm and weak absorptions in the 400–500 nm region, while excitation of **2** at 330 nm in acetonitrile gives an emission at 630 nm with a lifetime of 83 ns ($\Phi_{em} = 1.6 \times 10^{-4}$) at room temperature. The cyclic voltammograms of **1a** and **2** in acetonitrile consist of a quasi-reversible couple (-2.15 V vs. $Cp_2Fe^{0/+}$) and an irreversible wave ($+0.77$ V vs. $Cp_2Fe^{0/+}$). Both couples are assigned to ligand-centred processes. Reaction of Me_3TACN with $Cl(CO)_2py_2Cr{\equiv}CPh$ in THF resulted in cleavage of the carbyne moiety to yield a binuclear product. © 1998 Elsevier Science S.A.

Keywords: Carbyne complexes; Group 6 metals; Macrocyclic amine ligands; Photochemistry; Electrochemistry

1. Introduction

Investigation into the carbyne chemistry of Group 6 metals has proliferated in the last decade [1,2]. Many neutral carbyne complexes with facial monoanionic ligands of the type $[LM(CO)_2({\equiv}CR)]$ (M = Mo, W; R = alkyl, aryl, ferrocenyl; L = Cp, Cp* or indenyl [3–6], Tp (Tris(pyrazolyl)borate) [7,8], Tp* (Tris(3,5-dimethylpyrazolyl)borate) [9], $[(C_5H_5)Co\{P(O)R_2\}_3]$ [10]) have been studied. Amino and thio-stabilized derivatives have also been reported [11,12]. However, reports on cationic carbyne species are rare [13–15]; for example, Jamison et al. have described the synthesis and structure of the heteroatom-stabilized complex $[Tp^*W(CPMe_2Ph)(CO)_2]PF_6$ [16]. The ability of the tridentate macrocycles 1,4,7-trimethyl-1,4,7-triazacyclononane (Me_3TACN) and 1,4,7-triazacyclononane (TACN) to accommodate metal centres in high and low oxidation states is well documented [17–20]. The resultant complexes are evidently more stable than their acyclic congeners [21]. Herein is described the products from the reaction of $Cl(CO)_2py_2M{\equiv}CPh$ (M = Cr, Mo, W) with the triamine ligands and their structural, photophysical and electrochemical properties.

2. Results and discussion

Reaction of Me_3TACN or TACN with $Cl(CO)_2py_2Mo{\equiv}CPh$ in THF, followed by metathesis with sodium tetraphenylborate, afford the yellow complexes $[(Me_3TACN)Mo(CO)_2({\equiv}CPh)]BPh_4$ (**1a**) and $[(TACN)Mo(CO)_2({\equiv}CPh)]BPh_4$ (**1b**) respectively. Similarly, interaction of Me_3TACN with $Cl(CO)_2py_2W{\equiv}CPh$ yields $[(Me_3TACN)W(CO)_2({\equiv}CPh)]BPh_4$ (**2**) (Scheme 1). The ^1H and $^{13}C\{^1H\}$ NMR data suggest that complexes **1a**, **1b** and **2** contain a mirror plane along the metal–carbyne bond which bisects the triamine ligand and the two terminal carbonyl groups as expected. The high carbyne carbon chemical shifts in

---

[*] Corresponding author.

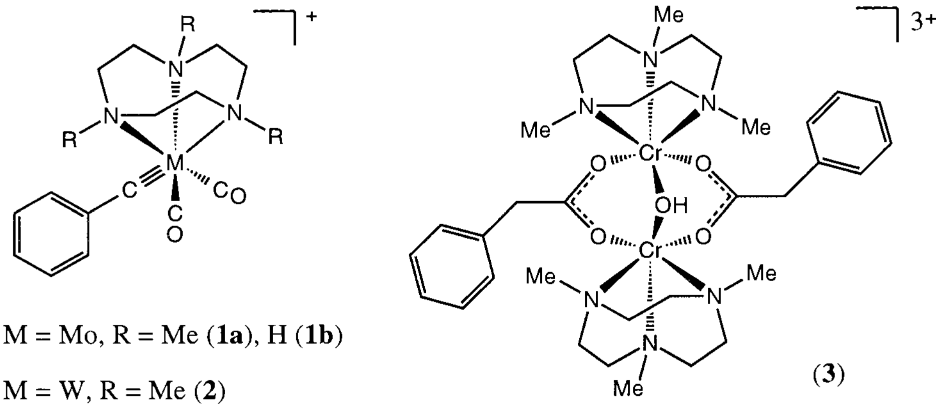

M = Mo, R = Me (**1a**), H (**1b**)

M = W, R = Me (**2**)

(**3**)

Scheme 1.

the $^{13}C\{^1H\}$ NMR spectra of **1a**, **1b** and **2** show that they are more electron-deficient than the terminal carbonyl carbons (Table 1).

The higher ν(CO) values in the IR spectrum of **1a** compared to **2** are consistent with the greater electron density associated with W at the same oxidation state. Complex **2** exhibits lower carbonyl stretching energies than other carbyne complexes of the respective metals listed in Table 1. This implies that the electron-donating strength of the ligands are in the order Me_3TACN > TACN > Tp ≥ Cp, and the metal centres of complexes containing Me_3TACN are more nucleophilic [15]. A comparison of ν(CO) in Table 1 shows that the carbyne moiety is a stronger π-acidic ligand than a terminal carbonyl, but weaker than a nitrosyl group in $[(Me_3TACN)Mo(CO)_2(NO)]^+$ and $[(Me_3TACN)W(CO)_2(NO)]^+$. We have therefore demonstrated that carbyne complexes can be prepared using pure σ-donor facial ligands.

Complexes **1a**, **1b** and **2** showed no observable changes after 3 months in aerobic dichloromethane, acetonitrile, acetone or water. Indeed, they are stable in the presence of concentrated HCl at ambient temperature for several hours. No reaction is observed upon treatment of **1a** or **2** with alkylating reagents such as PhLi and MeLi or $LiAlH_4$ in THF. Attempts to prepare carbonyl-free carbyne complexes from **1a** and **2** through substitution in refluxing neat $P(OMe)_3$ or by oxidation using bromine failed.

Since no cationic carbyne complexes containing purely σ-donor facial ligands have been structurally characterized, the X-ray crystal structures of **1a** and **2** have been determined (Table 2). The ORTEP plot of $[(Me_3TACN)Mo(CO)_2(\equiv CPh)]^+$ (**1a**) and the atomic numbering scheme are shown in Fig. 1. Selected bond distances and angles and atomic coordinates are collected in Tables 3 and 4. The molybdenum centre is in a distorted octahedral environment and is bonded to three

Table 1

Carbonyl stretching frequencies and selected $^{13}C\ \{^1H\}$ NMR data for Group 6 complexes containing Me_3TACN, TACN and related ligands

Complex	ν(CO)[a] (cm^{-1})	$\delta(M\equiv C)$(ppm)	$\delta(M{-}CO)$[d] (ppm)	References
$[(Me_3TACN)(CO)_2Mo\equiv CPh]^+$ (**1a**)	1980s, 1906s	298.0	225.2	
$[(TACN)(CO)_2Mo\equiv CPh]^+$ (**1b**)	1997s, 1914s	294.3	225.8	
$[(Me_3TACN)(CO)_2W\equiv CPh]^+$ (**2**)	1975s, 1879s	288.0	224.6	
$[Cp(CO)_2W\equiv CPh]$	1992s, 1922s[b]	299.3[e]	221.3[e]	[4]
$[Tp(CO)_2W\equiv CC_6H_4Me\text{-}4]$	1986s, 1903s[c]	284.8[f]	224.9[f]	[22]
$[(Me_3TACN)Mo(CO)_3]$	1880vs, 1750s			[20][g]
$[(Me_3TACN)W(CO)_3]$	1880vs, 1744s			[23][g]
$[(Me_3TACN)Mo(CO)_2(NO)]^+$	2010vs, 1920s			[23][g]
$[(Me_3TACN)W(CO)_2(NO)]^+$	1995vs, 1900s			[23][g]

[a] KBr unless specified otherwise.
[b] In *n*-hexane.
[c] In CH_2Cl_2.
[d] In d_6-acetone unless specified otherwise.
[e] In CD_2Cl_2.
[f] In CD_2Cl_2–CH_2Cl_2.
[g] $\delta(M{-}CO)$ not assigned.

Table 2
Crystal data for **1a** and **2**

	1a	**2**
Formula	$[C_{18}H_{26}N_3O_2Mo]$	$[C_{18}H_{26}N_3O_2W]$
Formula	$[C_{24}H_{20}B]$	$[C_{24}H_{20}B]$
Crystal system	Triclinic	Triclinic
Space group	$P\bar{1}$ (No. 2)	$P\bar{1}$ (No. 2)
a (Å)	13.216(2)	13.204(2)
b (Å)	14.331(4)	14.315(2)
c (Å)	10.774(2)	10.7754(9)
α (°)	96.56(2)	97.253(8)
β (°)	110.21(1)	110.231(9)
γ (°)	98.41(2)	98.54(1)
V (Å^3)	1864.2(8)	1854.9(4)
Z	2	2
M_r	731.60	819.51
d_c (g cm^{-1})	1.303	1.467
μ(Mo–Kα) (cm^{-1})	3.90	32.17
F(000)	764	828
T (K)	301	301
Refined parameters	442	442
R, wR	0.042, 0.051	0.031, 0.037

Me_3TACN nitrogen atoms, two terminal carbonyl ligands and one phenyl carbyne moiety. The Mo–C(3)–C(4) angle (174.7(5)°) and short Mo–C(3) bond (1.797(6) Å) are comparable to those in $Br(CO)_2py_2Mo{\equiv}CPh$ (165.5(5)° and 1.799(4) Å) [24]. Regarding the Mo–N(TACN) distances, the significantly longer Mo(1)–N(3) bond is attributed to the greater *trans* influence of the carbyne group [25]. The short Mo(1)–N(1) and Mo(1)–N(2) bonds are consistent with the high degree of back-bonding and relatively low ν(CO) values in **1a**. The long Mo(1)-N(3) bond also explains the deshielded $C_{carbyne}$ chemical shift in the $^{13}C\{^1H\}$ NMR spectrum.

The ORTEP plot of $[(Me_3TACN)W(CO)_2({\equiv}CPh)]^+$ (**2**) and the atomic numbering scheme are shown in Fig. 2. Selected bond distances and atomic coordinates are listed in Tables 5 and 6 respectively. The W(1)–C(3) distance of 1.800(6) Å and the W(1)–C(3)–C(4) angle of 174.4(4)° correspond to *sp*-hybridization at the C(3) carbon. In comparison with the carbyne bond distance (1.82(2) Å) and angle (176(2)°) in $Cp(CO)_2W{\equiv}CC_6H_4Me$-4 [5], it appears that the more electron-donating Me_3TACN ligand has little structural impact upon the metal–carbyne interaction. The relatively long W(1)–N(3) distance (2.316(5) Å) is again ascribed to the *trans* influence of the carbyne moiety.

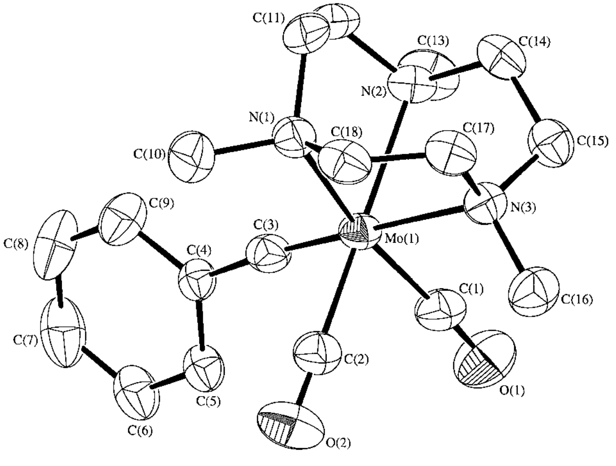

Fig. 1. ORTEP plot of $[(Me_3TACN)Mo(CO)_2({\equiv}CPh)]^+$ (40% probability ellipsoids).

Treatment of Me_3TACN with $Cl(CO)_2py_2Cr{\equiv}CPh$ yields the binuclear species $[(Me_3TACN)_2Cr_2^{III}(\mu\text{-}OH)(\mu\text{-}O_2CCH_2Ph)_2](PF_6)_3$ (**3**) as the major product (Scheme 1). The precise mechanism for its formation is unclear, although coupling of the carbyne and carbonyl ligands is apparently involved. Formation of new carbon–carbon bond by intramolecular carbonyl–carbyne coupling is rare in chromium chemistry [26]. The transformation also entails reduction of the metal centre, and in the absence of a reducing agent, the change in oxidation state may be the result of Cr(IV) disproportionation [27]. Isolation of the dinuclear complex $[(Me_3TACN)_2Cr_2^{III}(\mu\text{-}OH)(\mu\text{-}O_2CMe)_2]^{3+}$ has been reported [28]. A minor product isolated in 2% yield displays carbonyl stretching bands at 1980 and 1901 cm^{-1} in the IR spectrum and a molecular cluster at m/z 368 in the mass spectrum. These data correspond to the desired $[(Me_3TACN)Cr(CO)_2({\equiv}CPh)]^+$ fragment, but further characterisation was precluded due to its unstable nature.

The molecular structure of **3** has been determined, although the quality of data is poor (Section 4). The chromium atoms are linked by two $[PhCH_2CO_2]$ groups and one [OH] bridge while each metal centre is in a distorted octahedral environment and bonded to three nitrogen atoms of Me_3TACN. The $[PhCH_2CO_2]$ and [OH] bridging modes are similar to those in the related

Table 3
Selected bond lengths (Å) and angles (°) for **1a**

Mo(1)–C(1)	1.997(7)
Mo(1)–C(2)	1.976(7)
Mo(1)–C(3)	1.797(6)
Mo(1)–N(1)	2.276(4)
Mo(1)–N(2)	2.280(4)
Mo(1)–N(3)	2.351(4)
C(3)–C(4)	1.459(7)
C(1)–O(1)	1.146(7)
C(2)–O(2)	1.151(7)
Mo(1)–C(3)–C(4)	174.7(5)
Mo(1)–C(1)–O(1)	176.2(6)
Mo(1)–C(2)–O(2)	175.8(6)
N(1)–Mo(1)–C(1)	169.1(2)
N(2)–Mo(1)–C(2)	172.4(2)
N(3)–Mo(1)–C(3)	177.2(2)

Table 4
Atomic coordinates and B_{iso} / B_{eq} for **1a**

Atom	x	y	z	B_{eq}
Mo(1)	0.26237(4)	0.17040(4)	−0.00209(5)	3.42(1)
O(1)	0.3777(4)	0.0578(4)	−0.1635(5)	7.4(2)
O(2)	0.0891(4)	−0.0215(4)	−0.0902(5)	7.5(2)
N(1)	0.2008(4)	0.2435(3)	0.1488(5)	4.2(1)
N(2)	0.3882(4)	0.3107(3)	0.0845(4)	3.9(1)
N(3)	0.3797(4)	0.1424(3)	0.2047(4)	3.7(1)
C(1)	0.3385(5)	0.1016(5)	−0.1037(6)	4.8(2)
C(2)	0.1534(5)	0.0490(5)	−0.0526(6)	4.6(2)
C(3)	0.1781(5)	0.1916(4)	−0.1632(6)	3.9(1)
C(4)	0.1098(4)	0.1999(4)	−0.2989(5)	3.2(1)
C(5)	0.0925(5)	0.1262(4)	−0.4060(6)	4.0(1)
C(6)	0.0290(5)	0.1346(5)	−0.5343(6)	5.2(2)
C(7)	−0.0179(6)	0.2139(7)	−0.5570(7)	6.8(2)
C(8)	−0.0020(6)	0.2865(6)	−0.4532(8)	7.0(3)
C(9)	0.0614(6)	0.2789(5)	−0.3236(7)	5.2(2)
C(10)	0.0809(5)	0.2428(5)	0.0891(7)	5.9(2)
C(11)	0.2626(5)	0.3470(5)	0.2006(6)	5.0(2)
C(12)	0.3221(5)	0.3801(4)	0.1132(6)	4.8(2)
C(13)	0.4360(6)	0.3443(5)	−0.0136(7)	5.9(2)
C(14)	0.4809(5)	0.3042(5)	0.2109(6)	4.5(2)
C(15)	0.4884(5)	0.2012(5)	0.2230(6)	4.5(2)
C(16)	0.3883(5)	0.0407(5)	0.2022(6)	5.2(2)
C(17)	0.3409(5)	0.1741(4)	0.3148(6)	4.4(2)
C(18)	0.2220(5)	0.1857(5)	0.2575(6)	4.6(2)
C(19)	0.7794(4)	0.3835(4)	0.7207(5)	3.3(1)
C(20)	0.8815(5)	0.4319(4)	0.8155(6)	4.2(1)
C(21)	0.9535(5)	0.4979(5)	0.7843(7)	5.0(2)
C(22)	0.9274(5)	0.5186(5)	0.6576(8)	5.3(2)
C(23)	0.8277(6)	0.4719(5)	0.5602(6)	5.0(2)
C(24)	0.7577(5)	0.4050(4)	0.5922(6)	4.0(1)
C(25)	0.5667(4)	0.3111(4)	0.6865(5)	3.0(1)
C(26)	0.5316(5)	0.3915(4)	0.6401(6)	4.1(1)
C(27)	0.4214(5)	0.4027(5)	0.5985(6)	4.8(2)
C(28)	0.3425(5)	0.3284(6)	0.6021(6)	5.0(2)
C(29)	0.3735(5)	0.2481(5)	0.6450(6)	4.6(2)
C(30)	0.4826(5)	0.2387(4)	0.6880(5)	4.0(1)
C(31)	0.7166(4)	0.1995(4)	0.6849(5)	3.4(1)
C(32)	0.6432(5)	0.1376(4)	0.5707(6)	4.2(2)
C(33)	0.6696(6)	0.0561(5)	0.5149(6)	5.6(2)
C(34)	0.7700(6)	0.0319(5)	0.5749(7)	5.4(2)
C(35)	0.8435(5)	0.0904(5)	0.6879(8)	6.1(2)
C(36)	0.8185(5)	0.1713(5)	0.7425(7)	5.2(2)
C(37)	0.7215(4)	0.3044(4)	0.9130(5)	3.5(1)
C(38)	0.7231(6)	0.2245(5)	0.9753(6)	5.2(2)
C(39)	0.7387(6)	0.2285(5)	1.1098(7)	6.1(2)
C(40)	0.7539(5)	0.3143(6)	1.1895(6)	5.5(2)
C(41)	0.7519(5)	0.3948(5)	1.1349(7)	5.3(2)
C(42)	0.7357(5)	0.3894(4)	0.9985(6)	4.3(2)
B(1)	0.6958(5)	0.3001(5)	0.7511(6)	3.3(1)

complexes $[(TACN)_2Cr_2^{III}(\mu\text{-}OH)_2(\mu\text{-}CO_3)]^{2+}$ [29] and $[(TACN)_2Cr_2^{III}(\mu\text{-}OH)_2(\mu\text{-}SO_3)]^{2+}$ [19]. For example, the mean Cr–O(hydroxyl) distances in complex **3** and $[(TACN)_2Cr_2^{III}(\mu\text{-}OH)_2(\mu\text{-}CO_3)]^{2+}$ are 1.963 and 1.995 Å [29] respectively. There has been no previous report on structures containing the $PhCH_2CO_2$ moiety as a bridging ligand, although a structural account of the related derivative $[(Me_3TACN)_2Cr_2^{III}(\mu\text{-}O)(\mu\text{-}O_2CMe)_2]^{2+}$ (mean Cr–O(oxo) contacts 1.850 Å) has appeared [30].

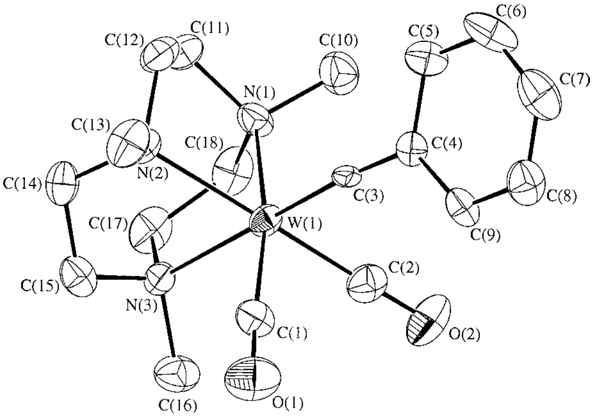

Fig. 2. ORTEP plot of $[(Me_3TACN)W(CO)_2(\equiv CPh)]^+$ (30% probability ellipsoids).

Complexes **1a**, **1b** and **2** exhibit intense absorption bands at 320–340 nm and weak absorptions in the 400–500 nm region (Fig. 3). The large extinction coefficients observed for the high energy bands at 324, 336 and 328 nm for **1a**, **1b** and **2** respectively suggest that they originate from charge transfer transitions [31], presumably MLCT. With reference to previous studies by Bocarsly et al. [32], Schoch et al. [33] and Xue et al. [31] on Mo(IV), W(IV) and Re(V) carbyne complexes, it is likely that the low energy absorptions at $\lambda > 400$ nm with low ε_{max} are due to a $d_{xy} \rightarrow d_\pi^*(d_{xz}, d_{yz})$ transition.

Excitation of complex **2** at 330 nm in acetonitrile gives an emission at 630 nm with a lifetime of 83 ns ($\Phi_{em} = 1.6 \times 10^{-4}$) at room temperature (Fig. 4). The large difference in emission and lowest allowed adsorption energies and the relatively long emission lifetime suggest that the transitions involved are due to spin-forbidden processes [33]. The emissive state is most likely to be $^3[(d_{xy})^1(d_\pi^*)^1]$.

Table 5
Selected bond lengths (Å) and angles (°) for **2**

W(1)–C(1)	1.969(8)
W(1)–C(2)	1.964(7)
W(1)–C(3)	1.800(6)
W(1)–N(1)	2.264(5)
W(1)–N(2)	2.266(5)
W(1)–N(3)	2.316(5)
C(3)–C(4)	1.456(8)
C(1)–O(1)	1.162(8)
C(2)–O(2)	1.163(8)
W(1)–C(3)–C(4)	174.4(4)
W(1)–C(1)–O(1)	177.1(6)
W(1)–C(2)–O(2)	175.7(7)
N(1)–W(1)–C(1)	171.7(2)
N(2)–W(1)–C(2)	168.9(2)
N(3)–W(1)–C(3)	178.1(2)

Table 6
Atomic coordinates and B_{iso}/B_{eq} for **2**

Atom	x	y	z	B_{eq}
W(1)	0.26225(2)	0.16814(2)	−0.00304(2)	3.339(7)
O(1)	0.0883(5)	−0.0255(4)	−0.0910(6)	7.5(2)
O(2)	0.3819(5)	0.0588(4)	−0.1612(6)	7.5(2)
N(1)	0.3879(4)	0.3083(3)	0.0871(5)	3.8(1)
N(2)	0.1995(4)	0.2403(4)	0.1471(5)	4.1(1)
N(3)	0.3777(4)	0.1429(3)	0.2019(5)	3.9(1)
C(1)	0.1535(6)	0.0462(5)	−0.0548(7)	4.8(2)
C(2)	0.3400(6)	0.1029(5)	−0.1022(6)	4.4(2)
C(3)	0.1764(4)	0.1884(4)	−0.1639(6)	3.4(1)
C(4)	0.1121(5)	0.1985(4)	−0.2999(6)	3.2(1)
C(5)	0.0656(6)	0.2805(5)	−0.3210(7)	5.0(2)
C(6)	0.0007(7)	0.2885(7)	−0.4502(10)	7.1(3)
C(7)	−0.0176(6)	0.2166(7)	−0.5557(9)	6.7(3)
C(8)	0.0270(6)	0.1366(6)	−0.5372(7)	5.4(2)
C(9)	0.0904(5)	0.1296(5)	−0.4088(6)	4.1(2)
C(10)	0.4361(6)	0.3427(5)	−0.0101(7)	5.6(2)
C(11)	0.3239(6)	0.3788(5)	0.1173(7)	4.9(2)
C(12)	0.2631(6)	0.3446(5)	0.2039(7)	5.0(2)
C(13)	0.0800(6)	0.2392(6)	0.0865(7)	5.7(2)
C(14)	0.2193(6)	0.1826(6)	0.2558(7)	5.3(2)
C(15)	0.3419(7)	0.1718(5)	0.3133(6)	5.5(2)
C(16)	0.3871(6)	0.0387(5)	0.1985(7)	5.5(2)
C(17)	0.4876(5)	0.1986(5)	0.2246(6)	4.6(2)
C(18)	0.4812(5)	0.3025(5)	0.2131(6)	4.5(2)
C(19)	0.7159(5)	0.2001(4)	0.6831(6)	3.7(2)
C(20)	0.6409(5)	0.1361(5)	0.5695(6)	4.2(2)
C(21)	0.6669(7)	0.0539(5)	0.5142(7)	5.7(2)
C(22)	0.7675(7)	0.0315(5)	0.5719(9)	5.7(2)
C(23)	0.8432(6)	0.0924(6)	0.6856(10)	6.0(2)
C(24)	0.8182(5)	0.1734(5)	0.7379(8)	5.6(2)
C(25)	0.7213(4)	0.3077(4)	0.9122(6)	3.5(1)
C(26)	0.7250(6)	0.2277(5)	0.9741(7)	5.5(2)
C(27)	0.7412(7)	0.2333(6)	1.1099(8)	6.7(2)
C(28)	0.7546(6)	0.3182(7)	1.1900(7)	5.6(2)
C(29)	0.7501(6)	0.3990(6)	1.1345(7)	5.1(2)
C(30)	0.7338(5)	0.3927(5)	0.9986(7)	4.4(2)
C(31)	0.5654(5)	0.3122(4)	0.6855(6)	3.3(1)
C(32)	0.4820(5)	0.2401(5)	0.6886(6)	3.9(2)
C(33)	0.3727(5)	0.2489(5)	0.6469(6)	4.5(2)
C(34)	0.3413(5)	0.3290(6)	0.6007(6)	4.7(2)
C(35)	0.4197(6)	0.4011(5)	0.5964(7)	4.6(2)
C(36)	0.5293(5)	0.3922(4)	0.6371(6)	3.9(2)
C(37)	0.7787(5)	0.3856(4)	0.7198(6)	3.4(1)
C(38)	0.8808(5)	0.4356(5)	0.8149(6)	4.3(2)
C(39)	0.9521(5)	0.5011(5)	0.7842(7)	5.0(2)
C(40)	0.9250(6)	0.5212(5)	0.6580(8)	5.2(2)
C(41)	0.8267(6)	0.4729(5)	0.5596(7)	4.6(2)
C(42)	0.7571(5)	0.4068(5)	0.5908(6)	4.0(2)
B(1)	0.6948(5)	0.3018(5)	0.7489(7)	3.4(2)

Bocarsly et al. [32] and Xue et al. [31] suggested that auxiliary ligands on carbyne complexes should have a significant effect on their luminescent properties. Kostic and Fenske [34] reported that the LUMO of Group 6 phenylcarbyne analogues are antibonding combinations of carbyne pπ– and metal dπ– orbitals and that UV–Vis radiation could promote metal-based electrons to the carbyne carbon. In this study, incorporation of a neutral macrocyclic ligand into the W(IV) cationic carbyne complex **2** causes a shorter-lived emissive state compared to neutral analogues [33]. Compounds **1a** and **1b** are not emissive in solution or solid state at room temperature.

Compounds **1a** and **2** exhibit identical electrochemical in acetonitrile; they are both reversibly reduced at −2.15 V vs. $Cp_2Fe^{0/+}$ and irreversibly oxidized at 0.77 V vs. $Cp_2Fe^{0/+}$. Metal-based processes are discounted since the redox potentials are independent of the metals. It is well established that Me_3TACN can tolerate drastic redox conditions [17]. Hence the irreversible wave is assigned to oxidation of the terminal carbonyl groups which leads to dissociation from the metal centres. The reversible couple is ascribed to a reduction centred at the phenyl ring. Complex **1b** exhibits only an irreversible wave at +0.86 V vs. $Cp_2Fe^{0/+}$ whereas **3** does not display any couples in the potential range accessible in acetonitrile.

3. Experimental details

3.1. General procedures

All operations were carried out using standard Schlenk techniques under an atmosphere of nitrogen. Diethyl ether, *n*-pentane and tetrahydrofuran were dried and distilled from sodium/benzophenone mixture. Dichloromethane (for reactions) was dried over phosphoric (V) oxide and stored in purified nitrogen, and (for photophysics) washed with concentrated sulphuric acid, 10% $NaHCO_3$ and water, then dried by $CaCl_2$ and distilled over CaH_2. Acetonitrile was distilled over $KMnO_4$ and then CaH_2. The compounds $[(CO)_5M{=}C(O)Ph][NMe_4]$ [35] (M = Cr, Mo, W) were prepared according to literature methods. Oxalyl chloride was used as received. Pyridine was freshly distilled from potassium hydroxide pellets prior to use. Compounds $Cl(CO)_2py_2M{\equiv}CPh$ (M = Cr, Mo, W) were prepared as described for the bromo analogue [36] except oxalyl chloride was used. TACN and Me_3TACN were prepared by literature methods [37].

Elementary analyses were performed by the Butterworth Laboratory, UK. IR spectra were recorded on a BIO-RAD FTS-7 FT IR spectrophotometer. ^{1}H, ^{13}C and ^{31}P NMR spectra were recorded on Bruker SPX300 or SPX500 Spectrometers. Chemical shifts were referenced to tetramethylsilane. Mass spectra were obtained from Finnigan Mat 95 mass spectrometer. UV–Vis absorption spectra were measured on a Perkin Elmer Lambda 19 UV–Vis–NIR spectrometer. Cyclic Voltammetry was performed on a Princeton Applied Research (PAR) model 273 potentiostat coupled to a Houseton 2000 x–y recorder. A conventional two compartment cell was used with silver–silver nitrate (0.1 mol dm^{-3}

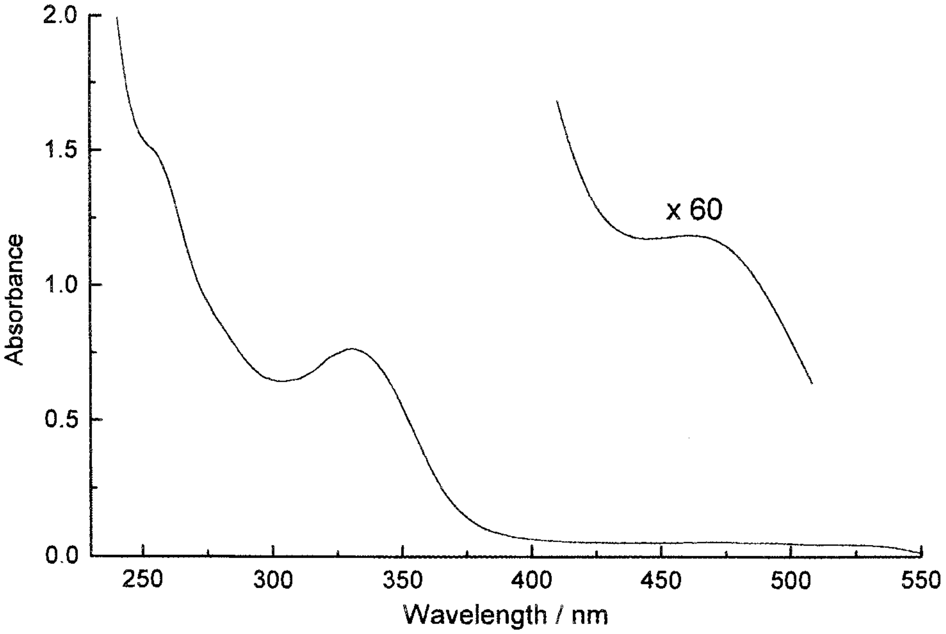

Fig. 3. UV–Vis spectrum of complex **2** (CH_2Cl_2).

in acetonitrile) as reference electrode. Ferrocenium–ferrocene ($Cp_2Fe^{0/+}$) couple was used as the internal standard. Edge-plane pyrolytic graphite and platinum were used as working and auxiliary electrodes respectively. Tetra-*n*-butylammonium hexafluorophosphate (0.1 mol dm^{-3}) was used as the supporting electrolyte. Steady-state emission spectra were recorded on a SPEX 1681 FLUOROLOG-2 series F111AI spectrometer. The emission lifetimes were determined and flash-photolysis measurements were performed with a Quanta Ray DCR-3 pulsed Nd-YAG laser system (pulse output 355 nm, 8 ns). The emission signals were detected by a Hamamatsu R928 photomultiplier tube and recorded on a Tektronix model 2430 digital oscilloscope.

3.2. *[(Me_3TACN)Mo(CO)$_2$(≡CPh)]BPh$_4$* ***(1a)***

To a solution of Me_3TACN (0.394 g, 2.3 mmol) in tetrahydrofuran (10 ml) was added Cl(CO)$_2$py$_2$Mo≡CPh (1.0 g, 2.3 mmol) and the resultant red solution was stirred at 50 °C for 8 h. After cooling, the yellow precipitate was collected by filtration and extracted into distilled water. Addition of a saturated aqueous solution of sodium tetraphenylborate to this afforded a yellow microcrystalline solid. Suitable crystals for X-ray crystallography were obtained from a dichloromethane–*n*-pentane solution at −20 °C. Yield: 1.35 g (80%). ^{1}H NMR (d$_6$-acetone): δ 7.54 (m, 2H, *o*-PhC), 7.47 (m, 1H, *p*-PhC), 7.40 (m, 2H, *m*-PhC), 7.28 (m, 8H, *o*-PhB), 7.00 (t, 8H, *m*-PhB), 6.84 (t, 4H, *p*-PhB), 3.50 (m, 4H, CH_2), 3.40 (s, 6H, CH_3), 3.37 (m, 4H, CH_2), 3.17 (m, 4H, CH_2), 2.94 (s, 3H, CH_3). ^{13}C{^{1}H} NMR(d$_6$-acetone): δ 298.0 (*C*Ph), 225.2 (*C*O), 146.1 (*ipso*-PhC), 136.7 (*o*-PhB), 131.0 (*o*-PhC), 130.0 (*m*-PhC), 129.5 (*p*-PhC), 126.6 (*m*-PhB), 122.7 (*p*-PhB), 60.1, 59.7, 57.7 (*C*H$_2$), 56.7, 51.4 (*C*H$_3$); IR ν_{CO}(KBr): 1982s, 1906s cm^{-1}. UV–Vis λ_{max}, nm (log ε) in CH_2Cl_2: 247 (4.34), 324 (3.96), 464 (2.08). Calc. for $C_{42}H_{46}N_3O_2BMo$ (M$_r$ 731.60): C, 68.95; H, 6.34; N, 5.74. Found: C, 69.12; H, 6.40; N, 5.58. FAB-MS: *m/z* 414 (M$^+$–BPh$_4$).

3.3. *[(TACN)Mo(CO)$_2$(≡CPh)]BPh$_4$* ***(1b)***

To a solution of TACN (0.130 g, 1.01 mmol) in THF (10 ml) was added Cl(CO)$_2$py$_2$Mo≡CPh (0.4 g, 0.92 mmol) at ambient temperature. The orange–yellow solution was stirred at 50 °C for 8 h. After cooling to ambient temperature, the yellow precipitate was collected and re-dissolved in warm water. The extract was treated with a saturated aqueous solution of NaBPh$_4$ to precipitate the product. This was filtered and recrystallized from acetone–*n*-pentane to yield a yellow crystalline product. Yield: 0.48 g (76%). ^{1}H NMR (d$_6$-acetone): δ 7.41 − 6.77 (m, 25H, PhC and PhB); 6.25 (br, 2H, N*H*); 4.92 (br, 1H, N*H*); 3.48 − 3.37 (m, 8H, CH_2CH_2); 3.15 − 2.94 (m, 4H, CH_2); ^{13}C {^{1}H} NMR(d$_6$-acetone): δ 294.3 (*C*Ph); 225.8 (*C*O); 146.1 (*ipso*-PhC); 136.7 (*o*-PhB); 130.1 (*o*-PhC); 129.7 (*m*-PhC); 129.1 (*p*-PhC); 126.6 (*m*-PhB); 122.7 (*p*-PhB); 49.9, 49.8, 47.7 (*C*H$_2$); ν_{CO}(KBr): 1997s, 1914s cm^{-1}; ν_{NH}(KBr): 3258s cm^{-1}; UV–Vis λ_{max}, nm (log ε) in CH_2Cl_2: 336 (3.98). Calc. for $C_{39}H_{40}N_3O_2BMo$ (M$_r$ 689.52): C, 67.94; H, 5.85; N, 6.09. Found: C, 68.02; H, 5.84; N, 5.98. FAB-MS: *m/z* 372 (M$^+$–BPh$_4$).

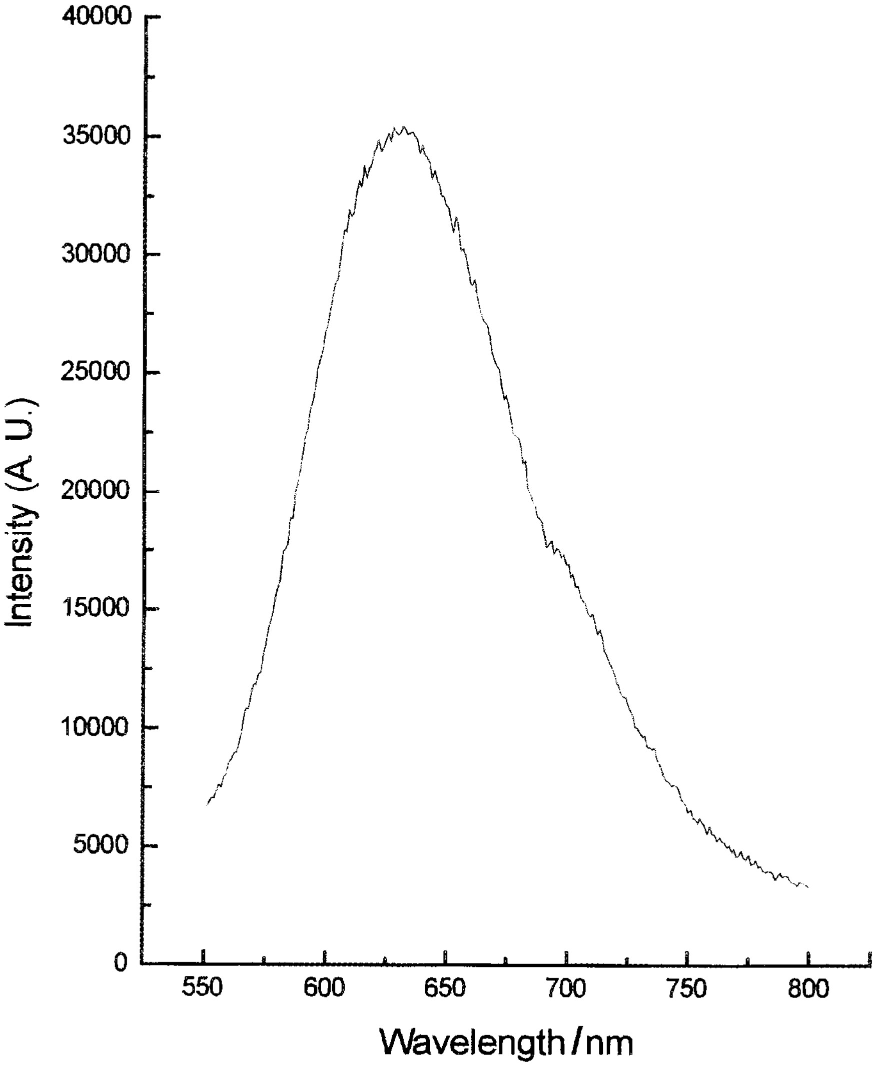

Fig. 4. Emission spectrum of complex **2** at room temperature (λ_{ex} = 330 nm, CH_3CN).

3.4. *[(Me_3TACN)W$(CO)_2$(≡CPh)]BPh_4 (2)*

A solution of Me_3TACN (0.654 g, 3.8 mmol) in tetrahydrofuran (10 ml) was added to a solution of $Cl(CO)_2py_2W{\equiv}CPh$ (2.0 g, 3.8 mmol) in tetrahydrofuran (10 ml) and the resulting red solution was stirred at 50°C for 6 h. The yellow precipitate formed was collected by filtration and dried in vacuo. The product was extracted into distilled water and treatment with a saturated aqueous solution of sodium tetraphenylborate afforded a yellow microcrystalline solid. Suitable crystals for X-ray crystallography were obtained from cooling of a dichloromethane–*n*-pentane solution. Yield: 2.66 g (85%). ^{1}H NMR (d_6-acetone): δ 7.40 (m, 5H, PhC), 7.28 (m, 8H, *o*-PhB), 7.00 (t, 8H, *m*-PhB), 6.84 (t, 4H, *p*-PhB), 3.95 (m, 4H, CH_2), 3.45 (s, 6H, CH_3), 3.37 (m, 4H, CH_2), 3.15 (m, 4H, CH_2), 2.92 (s, 3H, CH_3). ^{13}C{^{1}H} NMR (d_6-acetone): δ 288.4 (broad, *C*Ph), 224.6 (*C*O), 149.9 (*ipso*-PhC), 136.7 (*o*-PhB), 130.0 (*o*-PhC), 129.9 (*m*-PhC), 129.2 (*p*-PhC), 126.6 (*m*-PhB), 122.7 (*p*-PhB), 61.1, 60.6, 58.6 (CH_2), 57.6, 52.3 (CH_3); IR ν_{CO}(KBr): 1975s, 1879s cm^{-1}. UV–Vis λ_{max}, nm (log ε) in CH_2Cl_2: 250 (4.19), 328 (3.90), 462 (2.38). Calc. for $C_{42}H_{46}N_3O_2BW$ (M_r 819.51): C, 61.56; H, 5.66; N, 5.13. Found: C, 61.66; H, 5.80; N, 5.02. FAB-MS: m/z 500 (M^+–BPh_4).

3.5. *[(Me_3TACN)$_2Cr_2$(μ-OH)(μ-O_2CCH_2Ph)$_2$](PF_6)$_3$ (3)*

A solution of Me_3TACN (0.096 g, 0.56 mmol) in THF (10 ml) was added to a solution of $Cl(CO)_2py_2Cr{\equiv}CPh$ (0.20 g, 0.5 mmol) in THF at 0°C. The resulting solution was allowed to warm to ambient temperature and stirred for 2 days to give a pale green precipitate and green solution. The precipitate was filtered, washed with THF and re-dissolved in water. Solid NH_4PF_6 was added to the aqueous solution to precipitate a red product. Yield: 0.2 g (33%). Recrystallization at ambient temperature by diffusion of diethyl ether into an acetonitrile solution gave red crystals suitable for X-ray crystallography. ν_{CO} (Nujol): 1577 cm^{-1}. Calc. for $C_{34}H_{57}N_6O_5Cr_2F_{18}P_3$ (M_r 1168.78): C, 34.94; H, 4.92; N, 7.19. Found: C, 35.31; H, 5.06; N, 7.04. FAB-MS: m/z 358 ($[(Me_3TACN)Cr(PhCH_2CO_2)]^{2+}$).

3.6. Structural determination of **1a**

A pale yellow plate shaped crystal of dimensions $0.15 \times 0.10 \times 0.30$ mm was used for data collection at 301 K on a Rigaku AFC7R diffractometer with graphite monochromatized Mo–Kα radiation ($\lambda = 0.71073$ Å) using ω–2θ scans with ω-scan angle $(0.68 + 0.35 \tan \theta)°$ at a scan speed of 16.0 deg min^{-1} (up to 4 scans for reflection $I < 15\ \sigma(I)$). Intensity data (in the range of $2\theta_{max} = 45°$; h: 0 to 14; k: -15 to 15; l: -11 to 11 and 3 standard reflections measured after every 300 reflections showed decay of 1.27%), were corrected for decay and for Lorentz and polarization effects, and empirical absorption corrections based on the ψ-scan of four strong reflections (minimum and maximum transmission factors 0.945 and 1.000). Upon averaging the 5132 reflections, 4874 of which were uniquely measured, ($R_{int} = 0.048$), 3780 reflections with $I > 3\ \sigma(I)$ were considered observed and used in the structural analysis. The structure was solved by Patterson methods, expanded by Fourier methods (PATTY [38]) and refined by full-matrix least squares using the software package TeXsan [39] on a Silicon Graphics Indy computer. The 46 H atoms at calculated positions with thermal parameters equal to 1.3 times that of the attached C atoms were not refined. Convergence for 442 variable parameters by least squares refinement on F with $w = 4F_o^2/\sigma^2(F_o^2)$, where $\sigma^2(F_o^2) = [\sigma^2(I) + (0.010\ F_o^2)^2]$ for 6327 reflections with $I > 3\ \sigma(I)$ was reached at $R = 0.042$ and $wR = 0.051$ with a goodness-of-fit of 2.02. $(\Delta/\sigma)_{max} = 0.01$. The final difference Fourier map was featureless, with maximum positive and negative peaks of 0.59 and 0.66 e $Å^{-3}$ respectively.

3.7. Structural determination of **2**

A golden coloured, plate shaped crystal of dimensions $0.25 \times 0.07 \times 0.30$ mm was used for data collection at 301 K on a Rigaku AFC7R diffractometer with graphite monochromatized Mo–Kα radiation ($\lambda = 0.71073$ Å) using ω–2θ scans with ω-scan angle $(1.73 + 0.35 \tan \theta)°$ at a scan speed of 16.0 deg min^{-1} (up to 4 scans for reflection $I < 15\ \sigma(I)$). Intensity data (in the range of $2\theta_{max} = 45°$; h: 0 to 14; k: -15 to 15; l: -10 to 10 and 3 standard reflections measured after every 300 reflections showed no decay), were corrected for Lorentz and polarization effects, and empirical absorption corrections based on the ψ-scan of four strong reflections (minimum and maximum transmission factors 0.340 and 1.000). Upon averaging the 5095 reflections, 4844 of which were uniquely measured, ($R_{int} = 0.014$). 4362 reflections with $I > 3\sigma\ (I)$ were considered observed and used in the structural analysis. The structure was solved by heavy-atom Patterson methods, expanded using Fourier techniques [38] and refined by full-matrix least squares using the MSC-Crystal Structure Package TeXsan [39] on a Silicon Graphics Indy computer. The 49 non-H atoms were refined anisotropically and the 46H atoms at calculated positions with thermal parameters equal to 1.3 times that of the attached C atoms were not refined. Convergence for 442 variable parameters by least squares refinement on F with $w = 4F_o^2/\sigma^2(F_o^2)$, where $\sigma^2(F_o^2) = [\sigma^2(I) + (0.010\ F_o^2)^2]$ for 4362 reflections with $I > 3\sigma\ (I)$ was reached at $R = 0.031$ and $wR = 0.037$ with a goodness-of-fit of 2.46. $(\Delta/\sigma)_{max} = 0.05$. The final difference Fourier map was featureless, with maximum positive and negative peaks of 1.24 and 1.16 e $Å^{-3}$ respectively.

4. Supplementary material

Listings of crystal data and refinement, atomic coordinates, calculated coordinates, thermal parameters, bond lengths and angles and structure factors for **1a**, **2** and **3** are available as Supplementary Material from the authors.

Acknowledgements

We thank The University of Hong Kong and the Hong Kong Research Grants Council for financial support.

References

[1] H. Fischer, P. Hofmann, F.R. Kreissl, R.R. Schrock, U. Schubert, K. Weiss, Carbyne Complexes, VCH, Weinheim, 1988.

[2] A. Mayr, S. Ahn, Advances in Trans. Metal Coor. Chem., Vol. 1, JAI Press, London (1996) 1.

[3] H. Wadepohl, G.P. Elliott, H. Pritzkow, F.G.A. Stone, A. Wolf, J. Organomet. Chem. 482 (1994) 243.

[4] E.O. Fischer, T.L. Lindner, G. Huttner, P. Friedrich, F.R. Kreissl, J.O. Besenhard, Chem. Ber. 110 (1977) 3397.

[5] E. Delgado, J. Hein, J.C. Jeffery, A.L. Ratermann, F.G.A. Stone, L.J. Farrugia, J. Chem. Soc., Dalton Trans., (1987) 1191.

[6] S. Anderson, A.F. Hill, B.A. Nasir, Organometallics 14 (1995) 2987.

[7] F.R. Kreissl, J. Ostermeier, C. Ogric, Chem. Ber. 128 (1995) 289.

[8] Th. Lehotkay, K. Wurst, P. Jaitner, F.R. Kreissl, J. Organomet. Chem. 523 (1996) 105.

[9] B.E. Woodworth, J.L. Templeton, J. Am. Chem. Soc. 118 (1996) 7418.

[10] W. Kläui, T. Hardt, J. Organomet. Chem. 526 (1996) 313.

[11] A.C. Filippou, E.O. Fischer, W. Grünleitner, J. Organomet. Chem. 386 (1990) 333.
[12] A.C. Filippou, E.O. Fischer, J. Organomet. Chem. 341 (1988) C35.
[13] A.C. Filippou, B. Lungwitz, K.M.A. Wanninger, E. Herdtweck, Angew. Chem., Int. Ed. Engl. 34 (1995) 924.
[14] A.C. Filippou, D. Wössner, G. Kociok-Köhn, I. Hinz, L. Gruber, J. Organomet. Chem. 532 (1997) 207.
[15] R.A. Doyle, R.J. Angelici, Organometallics 8 (1989) 2207.
[16] G.M. Jamison, P.S. White, J.L. Templeton, Organometallics 10 (1991) 1954.
[17] P. Chaudhuri, K. Wieghardt, Prog. Inorg. Chem. 35 (1987) 329.
[18] K.S. Bürger, G. Haselhorst, S. Stötzel, T. Weyhermüller, K. Wieghardt, B. Nuber, J. Chem. Soc., Dalton Trans. (1993) 1987.
[19] P.T. Maragh, T.P. Dasgupta, D.J. Williams, J. Chem. Soc., Dalton Trans. (1995) 2843.
[20] G. Backes-Dahmann, W. Herrmann, K. Wieghardt, J. Weiss, Inorg. Chem. 24 (1985) 485.
[21] M.T.H. Tarafder, P. Bhattacharjee, A.K. Sarkar, Polyhedron 11 (1992) 795.
[22] M. Green, J.A.K. Howard, A.P. James, C.M. Nunn, F.G.A. Stone, J. Chem. Soc., Dalton Trans. (1986) 187.
[23] G.B. Backes-Dahmann, K. Wieghardt, Inorg. Chem. 24 (1985) 4044.
[24] H.S. Sun, X.Z. You, Y.Q. Yin, K.B. Yu, Polyhedron 13 (1994) 1475.
[25] A. Niemann, U. Bossek, G. Haselhorst, K. Wieghardt, B. Nuber, Inorg. Chem. 35 (1996) 906.
[26] P.F. Engel, M. Pfeffer, Chem. Rev. 95 (1995) 2281.
[27] E.S. Gould, Coord. Chem. Rev. 135/136 (1994) 651.
[28] P. Chaudhuri, M. Winter, H.J. Küppers, K. Wieghardt, B. Nuber, J. Weiss, Inorg. Chem. 26 (1987) 3302.
[29] K. Wieghardt, W. Schmidt, R. van Eldik, B. Nuber, J. Weiss, Inorg. Chem. 19 (1980) 2922.
[30] L.L. Martin, G. Blondin, J.J. Girerd, B. Nuber, J. Weiss, J. Chem. Soc., Chem. Commun. (1990) 1767.
[31] W.M. Xue, Y. Wang, T.C.W. Mak, C.M. Che, J. Chem. Soc., Dalton Trans. (1996) 2827.
[32] A.B. Bocarsly, R.E. Cameron, H.D. Rubin, G.A. Mc Dermott, C.R. Wolff, A. Mayr, Inorg. Chem. 24 (1985) 3976.
[33] T.K. Schoch, A.D. Main, R.D. Burton, L.A. Lucia, E.A. Robinson, K.S. Schanze, L. McElwee-White, Inorg. Chem. 35 (1996) 7769.
[34] N.M. Kostic, R.F. Fenske, Organometallics 1 (1982) 489.
[35] E.O. Fischer, A. Maasböl, Chem. Ber. 100 (1967) 2445.
[36] G.A. McDermott, A.M. Dorries, A. Mayr, Organometallics 6 (1987) 925.
[37] K. Wieghardt, P. Chaudhuri, B. Nuber, J. Weiss, Inorg. Chem. 21 (1982) 3086.
[38] PATTY: P.T. Beurskens, G. Admiraal, G. Beurskens, W.P. Bosman, S. Garcia-Granda, R.O. Gould, J.M.M. Smits, C. Smykalla, The DIRDIF program system, Technical Report of the Crystallography Laboratory, University of Nijmegen, The Netherlands (1992).
[39] TeXsan: Crystal Structure Analysis Package, Molecular Structure (1985 and 1992).